1 Introduction

Since many decades radar (RAdio Detection And Ranging) is used for the remote sensing of objects at far ranges and under adverse conditions like dust, snow or rain. Even though the initial idea dates back to 1904 [1], operational systems have been addressed starting from 1934 due to the potential military applications. Especially during the last 50 years a rapid development has occurred [2], that affected every single aspect of a radar sensor. While the operating frequency was pushed to higher bands, the signal generation changed from magnetron based approaches over waveguide circuits containing Gunn or IMPATT diodes to monolithic integrated and even multifunctional devices. Taking benefit from the general development of semiconductor devices in other fields, radar technology became affordable also in civil applications. Among those applications one can find space, air and ground based surveillance systems as well as industrial level gauging or simple motion sensors.

Within the last 30 years commercial mm-wave technology was mainly driven by the automotive industry. Having started at 24 GHz, the suppliers in Europe are now forced to switch to the 76–81 GHz frequency band due to administrative regulations. As a consequence, great efforts have been done in developing mm-wave components suitable for low cost mass production. Nowadays, chip sets or even single chip frontends are available, mainly based on GaAs or SiGe technology. Even though these devices are intended for automotive sensors, the technology is also available for fields with low volume and even niche applications. As an example the surveillance in harsh environments [3], the measurement of aircraft wake vortices [4, 5, 6], or the detection of foreign object debris (FOD) on airports [7] shall be mentioned.

With respect to radar signal processing, the availability of cost effective, high speed computers, analogue digital converters, and signal processors enables the transition of processing tasks from the analogue to the digital domain. Thereby, not only the radar processing itself, but also the antenna technology is concerned. Mechanically steered antennas and passive or active electronically steered antenna arrays are more and more replaced by digital beamforming (DBF) using multichannel sensors.

The application of such techniques has been demonstrated at a frequency of 24 GHz e.g. in [8, 9, 10], but there are several reasons to use higher frequencies. Aside from the before mentioned regulatory constraints, the bandwidth available at 79 GHz is much larger. Additionally, a higher antenna gain and narrower beamwidth can be achieved while maintaining the sensor dimensions. This fact makes this frequency range even more attractive for applications requiring a high resolution. However, when changing over to such high frequencies, several issues arise with respect to fabrication precision and cost.

The work described in this thesis deals with the development of a wideband sensor at 79 GHz suited to address many potential applications within different areas like industrial and security sensing. The main design goals are

- frequency modulated continuous wave (FM-CW) operation covering at least 5 GHz bandwidth,
- frontend with a single transmit and two receive channels,
- implementation of experimental options, e.g. for phase noise cancellation,
- switched antenna array extension for DBF operation,
- use of low cost printed circuit board technology and standard precision manufacturing.

Apart from the actual sensor design, the prediction of a system's performance has become an important issue to reduce the commercial risk of a product development. Especially at mm-wave frequencies the sensitivity of an FM-CW sensor is limited by the noise of the signal source. In [8] a computationally efficient approach is proposed to predict the influence of phase noise. The model described there includes some simplifications to accomplish a signal representation in terms of the instantaneous frequency. In order to overcome these simplifications, an instantaneous phase model will be derived in this work enhancing the accuracy without increasing the complexity.

Additionally, signal processing techniques will be developed coping with the large bandwidth and mitigating the effects of dynamic scenarios in conjunction with a switched antenna configuration. Finally, different sensor configurations will be validated in various exemplary applications such as the detection of FOD or environmental monitoring using synthetic aperture radar (SAR).

The thesis is organised in five chapters. After this introduction the fundamentals of the FM-CW radar are introduced in Chapter 2. Thereby, the basic means of intra pulse modulation and compression are treated as well as the signal processing in terms of range, Doppler shift, and digital beamforming. In Chapter 3 simulation and design aspects of the 79 GHz FM-CW frontend are presented together with an evaluation of the sensor performance. A description of the switched antenna array extension is found in Chapter 4. Due to the configuration of this array the generic DBF algorithms require some additional considerations, that are also addressed in this context. Simulation and measurement results demonstrate the capabilities of the switched array. Chapter 5 summarises some of the applications that have been investigated with the developed sensor hardware. The detection of FOD is described using, in a first step, mechanically steered sensors. The following part presents the results obtained with a SAR demonstrator setup, including typical operating modes such as stripmap SAR and spotlight SAR, but also three dimensional sensing by exploiting SAR and DBF. The conclusion in Chapter 6 gives a final summary of the work and discusses future developments enabled by new technologies such as MEMS or SiGe.

2 Fundamentals of Radar Principles and Signal Processing

By definition [11] radar (RAdio Detection And Ranging) uses the transmission and reception of electromagnetic waves to detect objects and extract their properties such as range and velocity. For example, the round trip delay of radio frequency pulses gives a measure of the target's distance. Fig. 2.1 shows the block diagram of a generic radar system consisting of waveform generator, receiver, and signal processing.

The shape of the pulses and the kind of reception help classifying radar systems. In the most simple case the transmitted waveform is a (rectangular) pulse without any intrinsic modulation. The duration or spatial extent of this pulse determines the range resolution. However, as shown later in this chapter, the maximum range of the radar is limited by the energy per pulse. Consequently, improving the resolution, while maintaining the peak power, reduces the maximum range. A common method to achieve a better resolution without affecting the maximum range is called pulse compression [11]. The exact meaning of this term will be discussed later. Basically, pulse compression is a technique to stretch the transmitted pulse in the time domain and to compress it during reception. This enables reducing the peak power that has to be provided by the transmitter.

Additionally, a distinction is drawn between coherent and non coherent radars.

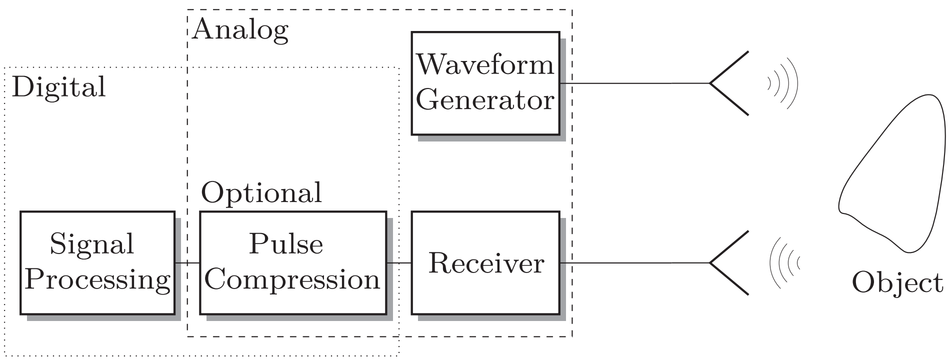

Fig. 2.1: Basic block diagram of a generic radar system.

In coherent radars the same oscillator or at least synchronous oscillators are used for waveform generation and down-conversion in the receiver, providing the phase relation between the transmitted and received pulses. It will be shown that this information is crucial for advanced processing methods such as digital beamforming (DBF). As this work deals with that kind of techniques, the further explanations will be restricted to coherent architectures.

2.1 Radar Principles

This sub-chapter gives a brief description of coherent pulse radars and introduces the principle of pulse compression and its relation to FM-CW (frequency modulated continuous wave) radars. As the latter one was used within this work, a detailed mathematical description follows together with considerations regarding signal processing.

2.1.1 Coherent Pulse Radars

The general principle of coherent pulse radars is shown in Fig. 2.2. The waveform is generated by modulating the output signal of an RF source (VCO, voltage controlled oscillator), and the same source serves as local oscillator (LO) for the receiver. By using two mixers with LO signals shifted by 90°, an in-phase and a quadrature channel is available at the output (I/Q receiver). By means

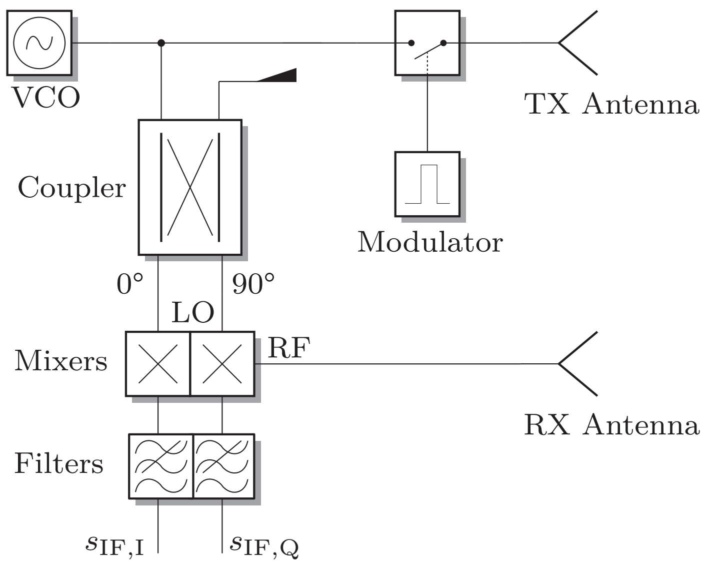

Fig. 2.2: Block diagram of a coherent pulse radar.

of this additional information the phase shift between the transmitted and received RF pulse can be measured at the intermediate frequency (IF) outputs ($s_{\mathrm{IF,I}}$ and $s_{\mathrm{IF,Q}}$) and used for further processing.

2.1.2 Analytical Description of the Radar Channel

Between transmitter and receiver the radar signal experiences a significant attenuation, mainly due to free space propagation. The relationship between transmitted and received power is known as the radar equation [12] and shall be shortly derived in the following. Assume a target located at a distance R in the farfield of the transmitting antenna. Using the transmitted power P_{TX} and the antenna gain G_{TX} the power density $S_{\mathrm{TX}}(R)$ at the target is

$$S_{\mathrm{TX}}(R) = \frac{P_{\mathrm{TX}} G_{\mathrm{TX}}}{4\pi R^2} \,. \tag{2.1}$$

A common way to describe the reflectivity of a target is in terms of the so-called radar cross section (RCS) σ. It is assumed that the power impinging on this hypothetical area σ is scattered uniformly to all directions. Hence, the power density at the location of the radar sensor caused by the scattered signal is

$$S_{\mathrm{RX}}(R) = \frac{S_{\mathrm{TX}}\sigma}{4\pi R^2} = \frac{P_{\mathrm{TX}} G_{\mathrm{TX}}\sigma}{(4\pi)^2 R^4} \,. \tag{2.2}$$

The effective area of the receiving antenna

$$A_{\mathrm{ant}} = G_{\mathrm{RX}} \frac{\lambda^2}{4\pi} \tag{2.3}$$

gives the relation between the incident power density and the power at the antenna output. Incorporating also the atmospheric attenuation α_{atm} which has a considerable influence especially at certain frequencies in the mm-wave range, the radar equation results in

$$P_{\mathrm{RX}}(R) = \frac{P_{\mathrm{TX}} G_{\mathrm{TX}} G_{\mathrm{RX}} \sigma \lambda^2}{(4\pi)^3 R^4} \cdot 10^{\frac{2\alpha_{\mathrm{atm}} \cdot R}{10}} \,. \tag{2.4}$$

In all radar systems the sensitivity, and consequently the ability to detect small targets, depends on the signal-to-noise ratio (SNR) after reception and pulse compression. The signal power can be calculated with the radar equation (2.4) whereas the noise power is given by the standard noise figure F_{RX} of the receiver:

$$P_{\mathrm{noise}} = k_B \left[T_{\mathrm{ant}} + (F_{\mathrm{RX}} - 1) T_0 \right] \Delta f_{\mathrm{IF}} \tag{2.5}$$

with k_B being the Boltzmann constant. For an antenna pointing to an environment with the temperature $T_0 = 290\,\mathrm{K}$, the equation can be simplified to

$$P_{\mathrm{noise}} = k_B T_0 F_{\mathrm{RX}} \Delta f_{\mathrm{IF}}. \tag{2.6}$$

The bandwidth Δf_{IF} relevant for the noise power calculation depends on the RF bandwidth ΔF and scales with the time-bandwidth product ($\mathrm{TBP} = T\,\Delta F$) of the transmitted pulse [11]:

$$\Delta f_{\mathrm{IF}} = \frac{\Delta F}{\mathrm{TBP}} = \frac{\Delta F}{T \Delta F} = \frac{1}{T} \tag{2.7}$$

Solving (2.4) for the maximum range at a given SNR yields

$$R_{\mathrm{max}} = \sqrt[4]{\frac{P_{\mathrm{TX}} T G_{\mathrm{TX}} G_{\mathrm{RX}} \sigma}{(4\pi)^3 k_B T_0 F_{\mathrm{RX}}\,\mathrm{SNR}}}\,. \tag{2.8}$$

In order to obtain a closed solution the atmospheric attenuation has been neglected. If this is not possible, e.g. for long range radars, the maximum range can be determined numerically.

2.1.3 Pulse Compression

In pulse radars the resolution in general is determined by the length or spatial extent of the transmitted pulse. If a better resolution and therefore a shorter pulse is required, the energy per pulse is reduced, if the peak power is kept constant. At the same time the signal-to-noise ratio decreases. A way to overcome this problem is using pulse modulation on transmit and pulse compression in the receiver.

Generic Description of Pulse Compression

The considerations in this section are following [11]. Complex analytical signals shall be used for the analysis. They allow the representation of arbitrary modulation schemes such as amplitude, phase, or frequency modulation in a consistent way. A generic modulated pulse can be expressed mathematically as

$$s_{\mathrm{TX}}(\tau) = s_{\mathrm{mod}}(\tau) \mathrm{e}^{\mathrm{j}\omega_0 \tau}\,, \tag{2.9}$$

where $\mathrm{e}^{\mathrm{j}\omega_0 \tau}$ represents the carrier and $s_{\mathrm{mod}}(\tau)$ the modulation signal. In the most simple case, the received pulse is a copy of the transmitted pulse delayed by $\Delta T = \frac{2R}{c_0}$ and weighted with a (in general complex) scalar value A. After down-conversion the baseband signal is

$$\tilde{s}_{\mathrm{mod}}(\tau) = A\, s_{\mathrm{mod}}(\tau - \Delta T)\,. \tag{2.10}$$

Pulse compression is done by correlating the received baseband signal with the transmitted template:

$$\begin{aligned} r_{s\tilde{s}}(\tau) &= A\, s^*_{\text{mod}}(-\tau) \star s_{\text{mod}}(\tau - \Delta T) \\ &= A \underbrace{s^*_{\text{mod}}(-\tau) \star s_{\text{mod}}(\tau)}_{\text{autocorrelation function } r_{ss}(\tau)} \star \delta(\tau - \Delta T) = A\, r_{ss}(\tau - \Delta T) \end{aligned} \quad (2.11)$$

According to (2.11) the response at the output of the pulse compression is the time-shifted autocorrelation function of the modulation signal. Hence, it is obvious, that the choice of the modulation signal strongly affects resolution and range sidelobes of the radar.

For radars without pulse compression the resolution is restricted to the temporal extent T of the transmitted (rectangular) pulse with a respective bandwidth $\Delta F = \frac{1}{T}$. Pulse compression techniques enable the use of waveforms occupying the same bandwidth but being considerably stretched in the time domain. The ability to compress such waveforms is given by their time-bandwidth product.

Common modulation schemes [12] are (non-)linear FM, pseudo random sequences, and, recently, even OFDM signals [13, 14]. Among these possibilities, linear FM radars play an important role as pulse compression can be partly shifted to the analogue domain. A discussion is given in the following section.

Application of Pulse Compression to Linear Frequency Modulated Pulses

A linear frequency-modulated transmit signal can be written as

$$s_{\text{TX}}(\tau) = s_{\text{mod}}(\tau) \mathrm{e}^{\mathrm{j}\omega_0 \tau} = \mathrm{e}^{\mathrm{j}\pi S \tau^2} \mathrm{e}^{\mathrm{j}\omega_0 \tau}\,, \quad (2.12)$$

where S denotes the slope of the frequency modulation in Hz/s. All considerations can be done in the baseband by omitting the carrier signal $\mathrm{e}^{\mathrm{j}\omega_0 \tau}$.

Due to free space propagation the modulation at the receiver input is delayed by $\Delta T = \frac{2R}{c_0}$:

$$\tilde{s}_{\text{mod}}(\tau) = s_{\text{mod}}(\tau - \Delta T) = \mathrm{e}^{\mathrm{j}\pi S (\tau - \Delta T)^2} \quad (2.13)$$

Again pulse compression is done by correlating the received pulse with the transmitted one:

$$
\begin{aligned}
r_{s\tilde{s}}(\tau) &= s^*_{\mathrm{mod}}(-\tau) \star \tilde{s}_{\mathrm{mod}}(\tau) \\
&= \int_{-\infty}^{\infty} s^*_{\mathrm{mod}}(-\tau')\tilde{s}_{\mathrm{mod}}(\tau-\tau')\mathrm{d}\tau' = \int_{-\infty}^{\infty} s^*_{\mathrm{mod}}(\tau')\tilde{s}_{\mathrm{mod}}(\tau+\tau')\mathrm{d}\tau' \\
&= \int_{-\infty}^{\infty} \tilde{s}_{\mathrm{mod}}(\tau')s^*_{\mathrm{mod}}(\tau'-\tau)\mathrm{d}\tau' \\
&= \int_{-\infty}^{\infty} \tilde{s}_{\mathrm{mod}}(\tau')\mathrm{e}^{-\mathrm{j}\pi S(\tau^2-2\tau\tau'+\tau'^2)}\mathrm{d}\tau' \\
&= \mathrm{e}^{-\mathrm{j}\pi S\tau^2} \int_{-\infty}^{\infty} \tilde{s}_{\mathrm{mod}}(\tau') \underbrace{\mathrm{e}^{-\mathrm{j}\pi S\tau'^2}}_{\text{Dechirp}} \underbrace{\mathrm{e}^{-\mathrm{j}2\pi(-S)\tau\tau'}}_{\text{Fourier transform}} \mathrm{d}\tau'
\end{aligned}
\qquad (2.14)
$$

Formally, in case of a linear frequency modulation the task of pulse compression can be split into a “dechirp” operation and a Fourier transform. After the dechirp the signal bandwidth is greatly reduced. Hence, an analogue implementation of this part is preferable, as the sampling rate of the ADC can be much lower. A possible solution is feeding the receiver with a chirped local oscillator signal. This is exactly what is done in FM-CW radars as described in Section 2.2.

2.2 Theory of FM-CW Radars

Fig. 2.3 shows a simplified block diagram of a frequency modulated continuous wave (FM-CW) radar. A voltage controlled oscillator (VCO) is used to generate a frequency modulated transmit signal. Neglecting dispersion, the received signal is simply an attenuated and delayed copy of the transmitted signal. Due to the frequency modulation there is a frequency offset between the VCO output and the receiver input. Using a linear modulation scheme as shown in Fig. 2.4 this frequency offset is constant. Hence, the output signal of the mixer is a harmonic signal. Using the definitions in Fig. 2.4 the slope of the linear frequency modulation is

$$S = \frac{\Delta F}{T} \qquad (2.15)$$

and the intermediate frequency results in

$$f_{\mathrm{IF}} = S \cdot \Delta T = S \cdot 2\frac{R}{c_0}\,, \qquad (2.16)$$

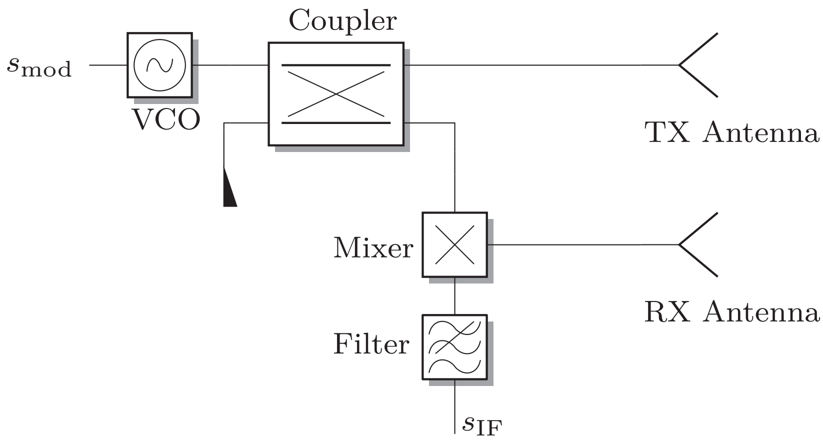

Fig. 2.3: Simplified block diagram of an FM-CW radar.

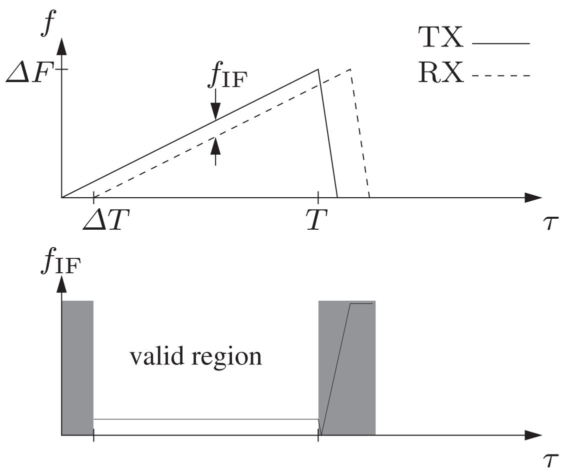

Fig. 2.4: Instantaneous frequency of transmitted (TX), received (RX) and intermediate frequency (IF) signal.

where ΔT is the round trip delay between sensor and target. Solving (2.16) for the target distance R yields

$$R = \frac{f_{\mathrm{IF}}\, c_0}{2S} \,. \tag{2.17}$$

According to (2.17) R is directly proportional to the intermediate frequency f_{IF}. Thus, for FM-CW radars the measurement of time delays is equivalent to a frequency measurement. For a larger number of targets the complete spectrum of the IF signal has to be estimated. Some possible methods are addressed in Section 2.3.

2.2.1 Mathematical Description of FM-CW Radars

The frequency domain description in the last paragraph neglects effects such as dispersion and modulation nonlinearities. Especially wideband FM-CW sensors are affected by these imperfections as they degrade the target response (point spread function) in terms of range resolution and sidelobes. To address as many effects as possible, a comprehensive model has to be set up in the time domain.

The instantaneous angular frequency at the output of a signal source with linear frequency modulation can be written as

$$\omega(\tau) = \omega_0 + 2\pi S\tau + e_{\mathrm{mod}}(\tau)\,, \tag{2.18}$$

where $e_{\mathrm{mod}}(\tau)$ contains the deviation from a perfectly linear modulation which will always occur in technical implementations. Considering also the phase noise $\phi_n(\tau)$ of the source, the instantaneous phase of the signal is

$$\begin{aligned}\phi_{\mathrm{SRC}}(\tau) &= \int\limits_{\tau'=0}^{\tau} \left(\omega_0 + 2\pi S\tau' + e_{\mathrm{mod}}(\tau')\right) \mathrm{d}\tau' + \phi_n(\tau) \\ &= \omega_0\tau + \pi S\tau^2 + \int\limits_{\tau'=0}^{\tau} e_{\mathrm{mod}}(\tau')\,\mathrm{d}\tau' + \phi_n(\tau) \\ &= \omega_0\tau + \pi S\tau^2 + \phi_e(\tau) + \phi_n(\tau)\,. \end{aligned} \tag{2.19}$$

Taking into account the over-all frequency response of the transmit path

$$H_{\mathrm{TX}}(\omega) = A_{\mathrm{TX}}(\omega)\mathrm{e}^{\mathrm{j}\phi_{\mathrm{TX}}(\omega)}\,, \tag{2.20}$$

the signal transmitted by the antenna is

$$\begin{aligned} s_{\mathrm{TX}}(\tau) &= A_{\mathrm{TX}}\big(\omega(\tau)\big)\cos\big[\phi_{\mathrm{SRC}}(\tau) + \phi_{\mathrm{TX}}\big(\omega(\tau)\big)\big] \\ &= A_{\mathrm{TX}}\big(\omega(\tau)\big)\cos\big[\omega_0\tau + \pi S\tau^2 + \phi_e(\tau) + \phi_n(\tau) + \phi_{\mathrm{TX}}\big(\omega(\tau)\big)\big] \end{aligned} \tag{2.21}$$

with the instantaneous angular frequency ω linked to τ according to (2.18).

The received signal is an attenuated copy of the transmitted signal, delayed by one round trip delay $\Delta T = 2\frac{R}{c_0}$ between sensor and target.

However, for a complete description also the frequency response of the receive path

$$H_{\mathrm{RX}}(\omega) = A_{\mathrm{RX}}(\omega)\cdot \mathrm{e}^{\mathrm{j}\phi_{\mathrm{RX}}(\omega)} \tag{2.22}$$

has to be considered. Hence:

$$\begin{aligned} s_{\mathrm{RX}} =& A_{\mathrm{RX}}\big(\omega(\tau-\varDelta T)\big)\, A_{\mathrm{TX}}\big(\omega(\tau-\varDelta T)\big)\cdot \\ & \cos\big[\phi_{\mathrm{SRC}}(\tau-\varDelta T) + \phi_{\mathrm{TX}}\big(\omega(\tau-\varDelta T)\big)+\phi_{\mathrm{RX}}\big(\omega(\tau-\varDelta T)\big)\big] \end{aligned} \tag{2.23}$$

For the modelling of the receiver a simplification is used. It is assumed that the frequency response of the mixer with respect to the local oscillator frequency does *not* depend on the actual intermediate frequency. Using this assumption the output signal of the receiver is

$$s_{\mathrm{IF}}(\tau) = s_{\mathrm{RX}}(\tau)\cdot A_{\mathrm{MXR}}\big(\omega(\tau)\big)\cos\big[\phi_{\mathrm{SRC}}(\tau) + \phi_{\mathrm{MXR}}\big(\omega(\tau)\big)\big]\,, \tag{2.24}$$

where $s_{\mathrm{RX}}(\tau)$ is the receiver input signal, $A_{\mathrm{MXR}}(\omega)$ the conversion loss as a function of the LO frequency, and $\phi_{\mathrm{MXR}}(\omega)$ the phase shift introduced by the mixer. Equation (2.24) can be rewritten as

$$\begin{aligned} s_{\mathrm{IF}}(\tau) =& A_{\mathrm{RX}}\big(\omega(\tau-\varDelta T)\big)\, A_{\mathrm{TX}}\big(\omega(\tau-\varDelta T)\big)\, A_{\mathrm{MXR}}\big(\omega(\tau)\big)\cdot \\ & \cos\big[\phi_{\mathrm{SRC}}(\tau-\varDelta T) + \phi_{\mathrm{TX}}\big(\omega(\tau-\varDelta T)\big)\big]\cdot \\ & \cos\big[\phi_{\mathrm{SRC}}(\tau) + \phi_{\mathrm{MXR}}\big(\omega(\tau)\big)\big]\,. \end{aligned} \tag{2.25}$$

Expanding (2.25) and omitting the high frequency signal components suppressed by the low pass behaviour of the IF section yields

$$\begin{aligned} s_{\mathrm{IF}}(\tau) =& A_{\mathrm{RX}}\big(\omega(\tau-\varDelta T)\big) A_{\mathrm{TX}}\big(\omega(\tau-\varDelta T)\big) A_{\mathrm{MXR}}\big(\omega(\tau)\big)\cdot && \text{AM} \\ & \cos\big[2\pi S\varDelta T\tau + \omega_0\varDelta T - \pi S\varDelta T^2 && \text{sinusoid} \\ & \left.\begin{aligned} &+ \phi_e(\tau) - \phi_e(\tau-\varDelta T) \\ &+ \phi_{\mathrm{MXR}}\big(\omega(\tau)\big) - \phi_{\mathrm{TX}}\big(\omega(\tau-\varDelta T)\big) \end{aligned}\right\} && \text{PM} \\ & + \phi_n(\tau) - \phi_n(\tau-\varDelta T)\big]\,. && \text{phase noise} \end{aligned} \tag{2.26}$$

Neglecting the frequency responses and the modulation nonlinearity in (2.26), the output signal of the receiver is a sinusoid, the frequency of which is directly related to the target distance.

Some interesting features can be derived from (2.26). All the system imperfections lead to a modulation of the desired sinusoidal signal in amplitude and phase. With respect to the modulation nonlinearity it can be seen that the influence almost cancels out for short delays $\varDelta T$ and low frequency components of $\phi_e(\tau)$. The same is true for the phase noise $\phi_n(\tau)$ and is known as an effect called phase noise cancellation. A detailed discussion is given in Section A.3 on page 130.